



Cite this: DOI: 10.1039/d4sc07995g

All publication charges for this article have been paid for by the Royal Society of Chemistry

# Rapid access to functionalized nanographenes through a palladium-catalyzed multi-annulation sequence†

Takehisa Maekawa \*<sup>a</sup> and Kenichiro Itami \*<sup>abc</sup>

Nanographenes and polycyclic aromatic hydrocarbons exhibit many intriguing physical properties and have potential applications across a range of scientific fields, including electronics, catalysis, and biomedicine. To accelerate the development of such applications, efficient and reliable methods for accessing functionalized analogs are required. Herein, we report the efficient synthesis of functionalized small nanographenes from readily available iodobiaryl and diarylacetylene derivatives *via* a one-pot, multi-annulation sequence catalyzed by a single palladium catalyst. This method enables the preparation of small nanographenes bearing various polar functional groups, such as hydroxy, amino, and pyridinic nitrogen atoms, which are otherwise difficult to incorporate. These functional groups provide valuable sites for further derivatization, allowing the modulation of small nanographenes' solubility, optoelectronic properties, and photochromic and vapochromic behaviors. Our new method thus provides a platform for facile access to novel carbon-based materials.

Received 25th November 2024

Accepted 4th January 2025

DOI: 10.1039/d4sc07995g

rsc.li/chemical-science

## Introduction

Nanographenes and polycyclic aromatic hydrocarbons (PAHs) are attractive compounds due to their unique optoelectronic properties, supramolecular behaviors, and potential applications across various fields.<sup>1</sup> Since their intrinsic properties are strictly defined by their shapes, sizes, and edge structures, the chemical synthesis of nanographenes and PAHs with atomic precision has attracted significant attention from the synthetic community over the past two decades.<sup>2</sup> These extensive investigations have led to the emergence of new synthetic techniques, such as annulative  $\pi$ -extension (APEX) reactions<sup>3,4</sup> and on-surface syntheses,<sup>5</sup> thereby enabling rapid access to structurally diverse nanographenes and PAHs.

In addition to significant progress in synthesizing fused aromatic hydrocarbons, their functionalized analogs are also attracting increasing interest (Fig. 1A).<sup>6</sup> Incorporating functional groups into nanographenes expands their range of applications in materials science and chemical biology by enabling the fine-tuning of photoelectronic properties, enhancing solubility, and allowing for the manipulation of

supramolecular interactions. For instance, Aida and Fukushima reported that hexa-*peri*-hexabenzocoronene derivatives bearing long aliphatic and tetramethylene glycol chains form supramolecular nanotube architectures, resulting in distinct

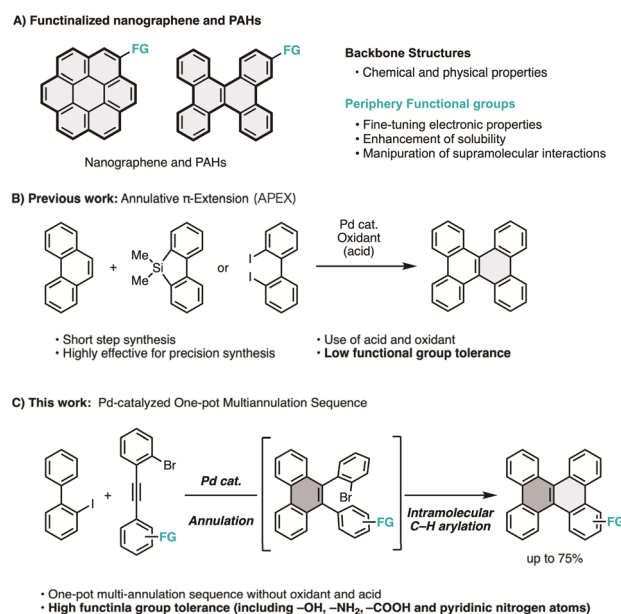


Fig. 1 Functionalized nanographenes and PAHs: (A) applications of functionalized nanographenes and PAHs. (B) Annulative  $\pi$ -extension reactions. (C) This work: Pd-catalyzed one-pot multi-annulation sequence. FG = functional group.

<sup>a</sup>Institute of Chemistry, Academia Sinica, 128 Academia Road, Section 2, Nankang, Taipei 115201, Taiwan. E-mail: tmaekawa@gate.sinica.edu.tw

<sup>b</sup>Molecule Creation Laboratory, Cluster for Pioneering Research, RIKEN, Wako, Saitama 351-0198, Japan. E-mail: kenichiro.itami@riken.jp

<sup>c</sup>Institute of Transformative Bio-Molecules (WPI-ITbM), Nagoya University, Chikusa, Nagoya 464-8602, Japan

† Electronic supplementary information (ESI) available. CCDC 2383473. For ESI and crystallographic data in CIF or other electronic format see DOI: <https://doi.org/10.1039/d4sc07995g>

photoconductivity and semiconducting properties.<sup>7</sup> Takimiya reported that a tetramethyl-thiolated pyrene exhibits ultrahigh charge mobility as a hole-transporting material in the crystal state.<sup>8</sup> Our group also found that a warped nanographene with tetraethylene glycol chains exhibited increased water solubility and induced cell death upon light irradiation.<sup>9</sup> Recently, Wilson reported that pyrene tethered to an osmium complex can be utilized for programmable surface modification of polymersomes.<sup>10</sup>

Although the significance of functional groups is clear, the synthesis of functionalized nanographene is not straightforward. General synthetic protocols used to access nanographenes and PAHs typically involve oxidative and/or acidic conditions, which typically result in low yields or no reaction when polar functionalities are incorporated into the substrates. Thus, available substituents are generally limited to nonpolar alkyl groups. Although the late-stage functionalization of nanographenes through halogenation,<sup>11</sup> iridium-catalyzed C–H borylation,<sup>12</sup> and APEX reactions<sup>3,4</sup> provide workable protocols, issues such as substrate-dependent regioselectivity and over-reaction limit the scope of these approaches to specific examples (Fig. 1B). Consequently, efficient and reliable methods for synthesizing functionalized nanographenes are in high demand.

Herein, we report a one-pot multi-annulation sequence for the synthesis of functionalized dibenzo[*g,p*]chrysene (DBC), a small nanographene motif, from 2-iodobiphenyls and diarylacetylenes using a single palladium catalyst (Fig. 1C). This simple yet powerful reaction enables the rapid synthesis of DBC derivatives bearing various polar functionalities, such as hydroxy groups, amino groups, and pyridinic nitrogen atoms. Additionally, we demonstrate how these functional groups can be utilized to modulate the solubility and photophysical properties of the functionalized DBCs through further derivatization.

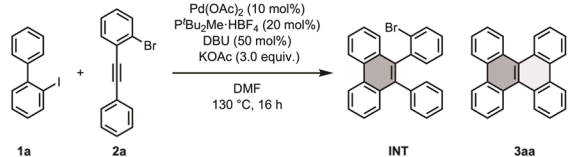
## Results and discussion

### Optimization of reaction conditions

Initially, we speculated that avoiding acidic or oxidative conditions would improve substrate tolerance when forming fused aromatic ring systems with polar functionalities. To establish a new efficient  $\pi$ -extension method with high functional group tolerance, we considered Larock's report, describing the annulation of 2-iodobiphenyl with internal alkynes to furnish 9,10-diarylphenanthrene using Pd(OAc)<sub>2</sub> and NaOAc under nearly neutral conditions.<sup>13</sup> Given that many palladium complexes are catalysts for constructing biaryl products,<sup>14,15</sup> we envisioned expanding palladium catalysis to a new  $\pi$ -extension reaction *via* a one-pot multi-annulation sequence of 2-iodobiaryls with appropriately designed diarylacetylenes, followed by intramolecular C–H arylation, to finally construct DBC frameworks.

We first identified the optimal conditions for forming DBC (**3aa**) using 2-iodobiphenyl (**1a**) and 1-bromo-2-(phenylethynyl) benzene (**2a**) as model substrates (Table 1). After extensive screening of reaction parameters, we discovered that **3aa** was efficiently formed in a 74% NMR yield and a 67% isolated yield

Table 1 Screening of reaction conditions for the one-pot multi-annulation sequence to synthesize DBC (**3aa**)<sup>a</sup>



Entry	Deviation from the optimum conditions	Yield <sup>b</sup> (%)	
		INT	<b>3aa</b>
1	None	n.d.	74 (67) <sup>c</sup>
2	Without P <sup>t</sup> Bu <sub>2</sub> Me·HBF <sub>4</sub>	64	23
3	PCy <sub>3</sub> ·HBF <sub>4</sub> instead of P <sup>t</sup> Bu <sub>2</sub> Me·HBF <sub>4</sub>	n.d.	66
4	P <sup>t</sup> Bu <sub>3</sub> ·HBF <sub>4</sub> instead of P <sup>t</sup> Bu <sub>2</sub> Me·HBF <sub>4</sub>	29	37
5	PPh <sub>3</sub> instead of P <sup>t</sup> Bu <sub>2</sub> Me·HBF <sub>4</sub>	43	25
6	2,2'-bipyridyl instead of P <sup>t</sup> Bu <sub>2</sub> Me·HBF <sub>4</sub>	49	29
7	Without KOAc	27	n.d.
8	K <sub>2</sub> CO <sub>3</sub> instead of KOAc	18	n.d.
9	KOPiv instead of KOAc	8	58
10	NaOAc instead of KOAc	24	53
11	Without DBU	n.d.	60
12	Et <sub>3</sub> N instead of DBU	n.d.	50
13	Pyridine instead of DBU	n.d.	63

<sup>a</sup> Conditions: **1a** (0.20 mmol), **2a** (1.5 equiv.), Pd(OAc)<sub>2</sub> (10 mol%), P<sup>t</sup>Bu<sub>2</sub>Me·HBF<sub>4</sub> (20 mol%), DBU (50 mol%), KOAc (3.0 equiv.), DMF (2.0 mL), 130 °C, 16 h. <sup>b</sup> NMR yield. CH<sub>2</sub>Br<sub>2</sub> was used as an internal standard. <sup>c</sup> Isolated yield.

when **1a** and **2a** were treated with Pd(OAc)<sub>2</sub>, P<sup>t</sup>Bu<sub>2</sub>Me·HBF<sub>4</sub>, 1,8-diazabicyclo(5.4.0)undec-7-ene (DBU), and KOAc in *N,N*-dimethylformamide (DMF) at 130 °C for 16 h (entry 1). During ligand screening, we observed that while the ligand did not influence the annulation step, it played a crucial role in the intramolecular C–H arylation. Without a ligand, the reaction halted at the first step, resulting in the mono-annulated product INT (entry 2). However, when electron-rich alkyl phosphine ligands such as PCy<sub>3</sub>·HBF<sub>4</sub> and P<sup>t</sup>Bu<sub>3</sub>·HBF<sub>4</sub> were employed, the reaction proceeded to yield the desired product (entries 3 and 4). Conversely, reactions with triphenylphosphine and 2,2'-bipyridyl resulted in low yields (entries 5 and 6). In addition to the ligands, the choice of additives was found to be crucial. When the reaction was performed without KOAc, no product **3aa** was observed, and a significant reduction in the amount of the intermediate (INT) was noted (entry 7). Similarly, using K<sub>2</sub>CO<sub>3</sub> instead of KOAc resulted in no formation of **3aa** and a reduced yield of INT (entry 8). Comparable yields were obtained when KOPiv or NaOAc were used instead of KOAc (entries 9 and 10), indicating that carboxylate anions are essential for C–H activation and annulation. The addition of DBU slightly enhanced the yield of **3aa**, whereas its absence led to a reduction in yield (entry 11). Other organic bases, such as triethylamine (Et<sub>3</sub>N) and pyridine, did not influence the yield (entries 12 and 13). We postulate that DBU contributes to the efficient generation of active Pd species from the precatalyst or neutralizes the acetic acid generated during the C–H activation steps.



## Scope of substrates

Having established the optimal reaction conditions, we assessed the scope of the reaction with respect to  $\pi$ -extending agents (Fig. 2). We first evaluated  $\pi$ -extending agents bearing *para*-functionalized arenes and found that various functional groups were compatible with this one-pot multi-annulation process. The reaction with the methoxy-substituted  $\pi$ -extending agent **2b** yielded the corresponding product **3ab** in 70% yield. The acetoxy group, which is susceptible to hydrolysis under basic conditions, afforded the deacetylated product **3ac** directly in 69% yield. The  $\pi$ -extending agent bearing a non-protected amine (**2d**), a challenging functional group in Pd catalysis, furnished DBC-NH<sub>2</sub> (**3ad**) in 30% yield. Electron-withdrawing substituents such as Cl, CN, and CF<sub>3</sub> groups were also tolerated, delivering the corresponding products in yields of 62–75% (**3ae–ag**). We then explored  $\pi$ -extending agents with *meta*-substituted arenes (2h–k). For substrates with electron-donating groups, the corresponding products **3ah–ak**

were afforded as mixtures of separable regioisomers, often in equal or higher yields compared to those with *para*-substituted  $\pi$ -extending agents. In contrast to the general regioselectivity observed in C–H activation *via* the concerted metalation-deprotonation (CMD) pathway,<sup>15</sup> which typically favors the most acidic or sterically accessible C–H bond, the sterically hindered product was obtained as the major isomer. This trend in reactivity and regioselectivity can be attributed to the proximal guidance by the coordinating functional groups during the C–H activation process.<sup>16</sup> In contrast, electron-withdrawing groups, such as acetyl and carboxylic acids, exhibited the opposite regioselectivity, likely due to increased steric hindrance. The compatibility of coordinative heteroaromatic rings is notable; reactions with  $\pi$ -extending agents bearing 4-pyridyl (**2l**), 3-pyridyl (**2m**), 5-pyrimidyl (**2n**), and 3-quinolinyl (**2o**) produced the corresponding aza-DBC's **3al–ao** in good yields, in the range of 47–75%. Further investigations focused on utilizing the present method to construct larger structures

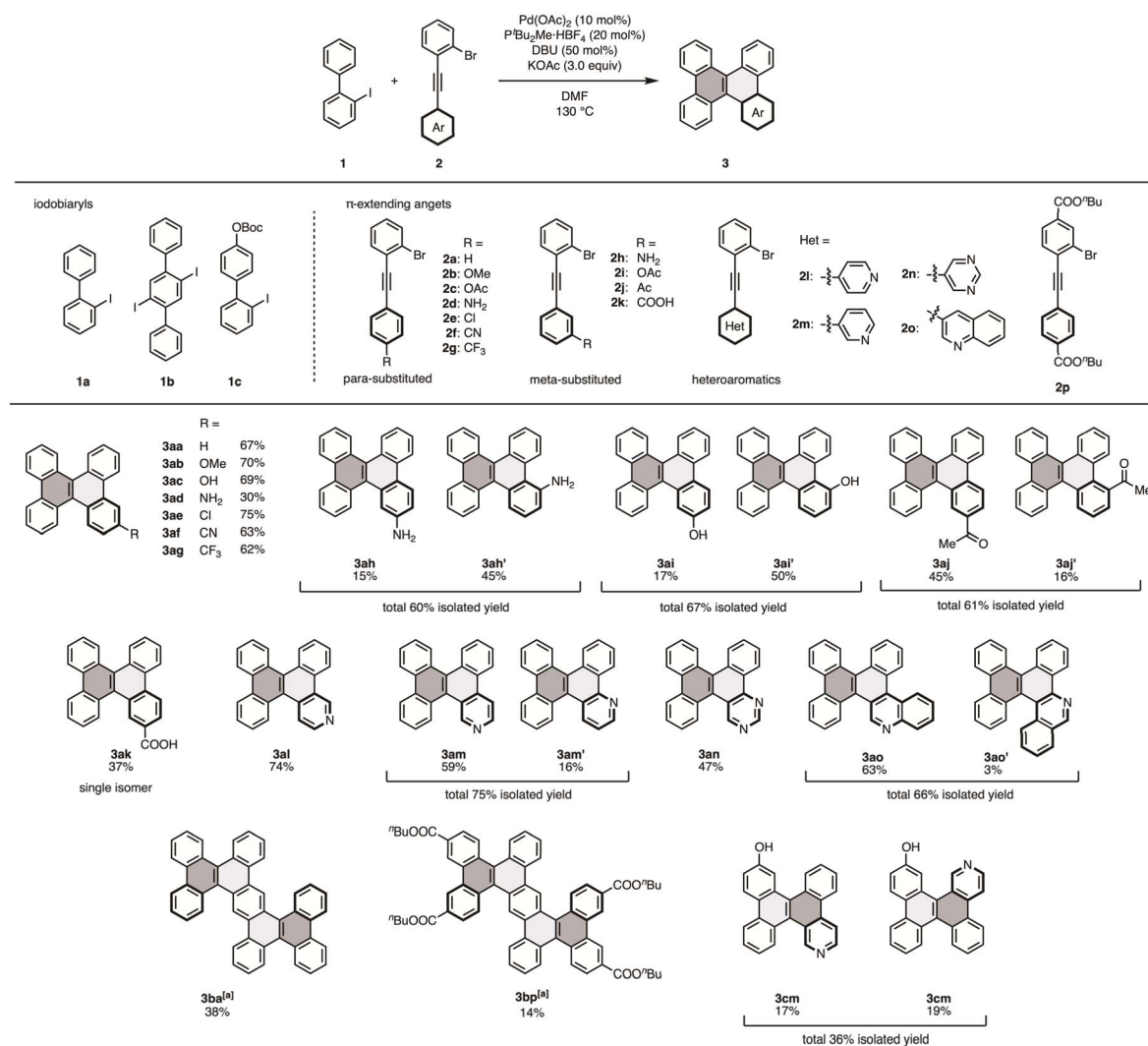


Fig. 2 Scope of substrates for the Pd-catalyzed one-pot multi-annulation sequence. Conditions: (1) (0.20 mmol, 1.0 equiv.), (2) (1.5 equiv.), Pd(OAc)<sub>2</sub> (10 mol%), P<sup>t</sup>Bu<sub>2</sub>Me·HBF<sub>4</sub> (20 mol%), DBU (50 mol%), KOAc (3.0 equiv.), DMF (2.0 mL), 130 °C, 16 h. <sup>a</sup>3.0 equiv.  $\pi$ -extending agent, 20 mol% Pd(OAc)<sub>2</sub>, 40 mol% P<sup>t</sup>Bu<sub>2</sub>Me·HBF<sub>4</sub>, 1.0 equiv. DBU were used.



and bifunctionalized derivatives. When 2',5'-diiodo-1,1':4',1''-terphenyl (**1b**) was employed instead of **1a**, the reaction with **2a** afforded the doubly extended product **3ba** in 38% yield. Moreover, its functionalized analog **3bp** was synthesized *via* the double  $\pi$ -extension of **1b** with **2p**, although in a low yield. Boc-protected substrate **1c** reacted with **2m** to yield bifunctional DBC analogs **3cm** and **3mc'** as deprotected forms, in 17% and 19% yields, respectively. Overall, this novel  $\pi$ -extension method exhibits broad functional versatility and holds potential for the synthesis of a range of functionalized nanographene structures.

### Further derivatization of **3ah'** and **3cm**

The properties of functionalized DBCs can be further modified through additional derivatization (Fig. 3). For instance, aminated DBC **3ah'** was reacted with carboxylic acid *via* a general condensation procedure to yield **3ah'-amide** in 82% yield. Unlike unfunctionalized DBC, **3ah'-amide** remained in a liquid state at room temperature and displayed improved solubility in polar solvents. Furthermore, **3ah'** was coupled with 4-iodoaniline after nitrosation with *m*-chloroperbenzoic acid (mCPBA), producing **3ah'-azobenzene**, which has potential applications in photoswitching materials. The Sandmeyer reaction was also used to convert **3ah'** into iodinated DBC **1d** with a yield of 62%. This iodinated DBC was then used in a multi-annulation sequence with **2l**, resulting in **3dl** in 10% yield; **3dl** is a heterocyclic analog of hexabenzocyclopentene (HBT), known for its excellent hole-transporting properties in OLEDs.<sup>17</sup> In addition, **3am** was functionalized with various alkyl electrophiles to form ionic DBCs. Reaction with mPEG4Br produced **3am-PEG4<sup>+</sup>Br<sup>-</sup>** as a gel-like yellow semisolid in quantitative

yield. Treatment with 1,6-dibromohexane resulted in the formation of the ionic dimer **3a** in 74% yield. A similar protocol was applied for bifunctional DBC **3cm**, yielding the zwitterionic species **3cm-Me**. Among these ionic DBC derivatives, **3am-PEG4<sup>+</sup>Br<sup>-</sup>** displayed excellent solubility in various organic solvents and aqueous media. This dramatic enhancement in solubility can be attributed to the ionic nature of the pyridinium moiety and the hydrophilic triethylene glycol chain.

### Photophysical properties of functionalized DBCs

Selected UV-vis absorption spectra of the functionalized DBCs in dry DMF solution ( $6.87\text{--}7.50 \times 10^{-5}$  M) are shown in Fig. 4. Compounds **3am** and **3cm** displayed intense absorption bands with the longest absorption maxima at 352 and 355 nm, respectively (Fig. 4 and ESI). These absorption profiles closely resemble those of the parent DBC in dichloromethane solution,<sup>18</sup> indicating that nitrogen-doping and hydroxylation have minimal impact on the DBC structure's absorption characteristics. In contrast, **3am-PEG4<sup>+</sup>Br<sup>-</sup>** exhibited a red-shifted absorption band, with the longest wavelength absorption maximum at 421 nm. DFT calculations at the B3LYP/6-31+G(d) level estimated the HOMO and LUMO energy levels of **3am** to be  $-5.761$  eV and  $-1.94$  eV, respectively, while for **3am-PEG4<sup>+</sup>Br<sup>-</sup>**, the values were  $-8.722$  eV and  $-5.791$  eV (see ESI<sup>†</sup>). The red-shifted absorption is likely due to a significant decrease in the LUMO energy level relative to the HOMO upon *N*-alkylation, leading to a narrow HOMO–LUMO energy gap. In addition, **3cm-Me** showed a further red-shifted absorption band with a weak broad absorption between 480 and 700 nm, attributed to intramolecular charge transfer.<sup>19</sup> This weak absorption band

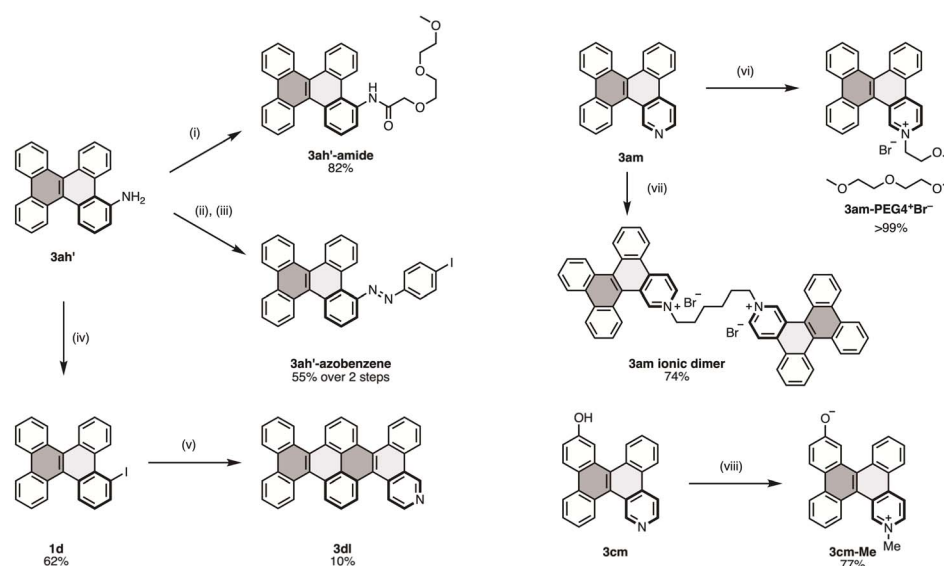


**Fig. 3** Further derivatization of **3ah'** and **3am**. (i) [2-(2-methoxyethoxy)ethoxy]acetic acid (3.0 equiv.), HCTU (3.0 equiv.), Et<sub>3</sub>N (5.7 equiv.), DMF, rt, 26 h, 82% yield; (ii) mCPBA (3.1 equiv.), toluene, rt, 0.5 h, 81% yield; (iii) 4-iodoaniline (3.0 equiv.), CH<sub>2</sub>Cl<sub>2</sub>/AcOH, 60 °C, 24 h, 68% yield; (iv) NaNO<sub>2</sub> (1.7 equiv.), conc. HCl, 0 °C, 2 h, then KI (10 equiv.), rt, 12 h, 62% yield; (v) **2l** (1.7 equiv.), Pd<sub>2</sub>(dba)<sub>3</sub>·CHCl<sub>3</sub> (5 mol%), KOAc (3.0 equiv.), DMF, 130 °C, 12 h, then additional Pd<sub>2</sub>(dab)<sub>3</sub>·CHCl<sub>3</sub> (5 mol%), P<sup>t</sup>Bu<sub>2</sub>Me·HBF<sub>4</sub> (40 mol%), DBU (1.0 equiv.), 150 °C, 3.5 h, 10% yield; (vi) mPEG4Br (3.9 equiv.), DMF, 90 °C, 20 h, >99% yield; (vii) 1,6-dibromohexane (0.5 equiv.), DMF, 90 °C, 12 h, 74% yield; (viii) MeI (1.1 equiv.), DMF, 90 °C, 2.5 h, then NBu<sub>4</sub>OH (1.0 equiv.), MeOH/DMSO, 5 min, 77% yield. HCTU = 2-(6-chloro-1*H*-benzotriazole-1-yl)-1,1,3,3-tetramethylammonium hexafluorophosphate; dba = dibenzylideneacetone; mPEG4Br = triethylene glycol 2-bromoethyl methyl ether.



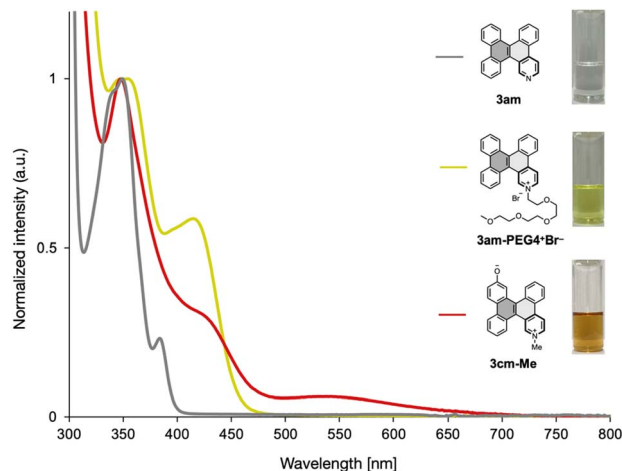


Fig. 4 UV-vis absorption spectra of **3am**, **3am-PEG4<sup>+</sup>Br<sup>-</sup>**, and **3cm-Me** in dry DMF solution.

was attenuated when a mixture of dry DMF and H<sub>2</sub>O (99 : 1, v/v) was used as the solvent, and was completely diminished in a DMF/AcOH (99 : 1, v/v) solution (Fig. 5A). Sensitivity to water and acid was even more pronounced in the solid state (Fig. 5B). The solid form of **3cm-Me** changed color from dark brown to orange when exposed to atmospheric moisture and reverted to dark brown after 30 min under vacuum. Upon exposure to AcOH vapor, the orange solid of **3cm-Me** irreversibly turned yellow, corresponding to the protonated state. This vapochromic behavior in response to humidity and acid vapor demonstrates the potential of **3cm-Me** as a vapor-sensing material.<sup>20</sup>

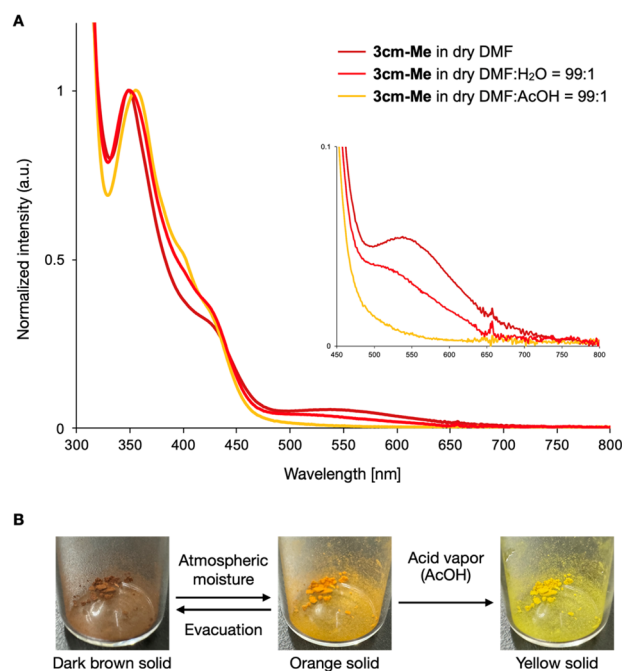


Fig. 5 Water and acid response behavior of **3cm-Me**. (A) Water and acid responsive absorption changes in solution. (B) Moisture and acid vapor responsive color changes in the solid state.

## Conclusions

In summary, we established an efficient approach for functionalizing nanographenes and PAHs *via* a Pd-catalyzed one-pot, multi-annulation sequence. The combination of Pd(OAc)<sub>2</sub>/P<sup>t</sup>Bu<sub>2</sub>Me·HBF<sub>4</sub>/KOAc effectively promotes both the annulation of 2-iodobiphenyls with diarylacetylenes and subsequent intramolecular C–H arylation, leading to the formation of the DBC framework. The high functional group tolerance of this one-pot sequence allows rapid access to a range of functionalized DBCs bearing amino, hydroxy, and carboxylic acid groups, as well as pyridinic nitrogens—compounds that are challenging to synthesize using previous  $\pi$ -extension methods. We also demonstrated that these functional groups serve as reliable reactive sites for further derivatization, yielding azobenzene, azanographene, and ionic DBCs. UV-vis absorption spectra and DFT calculations of the ionic DBCs indicate that *N*-alkylation significantly affects their photophysical properties. Additionally, we revealed the unique vapochromic properties of the zwitterionic DBC. Overall, the method developed in this study serves as a reliable platform for facile access to novel carbon-based materials.

## Data availability

The data supporting the findings of this study are available in the ESI material.†

## Author contributions

T. M. and K. I. conceived and designed the research. T. M. performed experiments and collected the data. T. M. and K. I. wrote the manuscript.

## Conflicts of interest

The authors declare no conflict of interest.

## Acknowledgements

We thank Mr Jia-Wei She and Dr Hsiao-Hua Yu (Academia Sinica) for their support with the UV-vis absorption measurements. We also thank Mr Daiki Imoto and Associate Prof. Akiko Yagi (Nagoya University) for their support with the DFT calculations. This study was supported by the Ministry of Science and Technology of Taiwan and Academia Sinica (grant number AS-GC-111-M05). Computational studies were conducted at the Research Center for Computational Science in Okazaki, Japan (24-IMS-C123). Mass spectrometry analyses were performed by Mass Spectrometry facility of the Institute of Chemistry, Academia Sinica, Taiwan.

## Notes and references

- For selected reviews on the application of nanographenes and graphene nanoribbons, see: (a) V. Georgakilas, J. A. Perman, J. Tucek and R. Zboril, *Chem. Rev.*, 2015, **115**,



- 4744; (b) N. Panwar, A. M. Soehartono, K. K. Chan, S. Zeng, G. Xu, J. Qu, P. Coquet, K.-T. Yong and X. Chen, *Chem. Rev.*, 2019, **119**, 9559; (c) Y. Gu, Z. Qiu and K. Müllen, *J. Am. Chem. Soc.*, 2022, **144**, 11499.
- 2 (a) Y. Segawa, H. Ito and K. Itami, *Nat. Rev. Mater.*, 2016, **1**, 15002; (b) Y. Segawa, A. Yagi, K. Matsui and K. Itami, *Angew. Chem., Int. Ed.*, 2016, **55**, 5136; (c) K. Itami and T. Maekawa, *Nano Lett.*, 2020, **20**, 4718; (d) I. A. Stepek, M. Nagase, A. Yagi and K. Itami, *Tetrahedron*, 2022, **123**, 132907.
- 3 For reviews on APEX reactions, see: (a) H. Ito, K. Ozaki and K. Itami, *Angew. Chem., Int. Ed.*, 2017, **56**, 11144; (b) H. Ito, Y. Segawa, K. Murakami and K. Itami, *J. Am. Chem. Soc.*, 2019, **141**, 3.
- 4 (a) K. Mochida, K. Kawasumi, Y. Segawa and K. Itami, *J. Am. Chem. Soc.*, 2011, **133**, 10716; (b) K. Ozaki, K. Kawasumi, M. Shibata, H. Ito and K. Itami, *Nat. Commun.*, 2015, **6**, 6251; (c) K. Ozaki, K. Murai, W. Matsuoka, K. Kawasumi, H. Ito and K. Itami, *Angew. Chem., Int. Ed.*, 2017, **56**, 1361; (d) W. Matsuoka, H. Ito and K. Itami, *Angew. Chem., Int. Ed.*, 2017, **56**, 12224; (e) Y. Koga, T. Kaneda, Y. Saito, K. Murakami and K. Itami, *Science*, 2018, **359**, 435; (f) S. Matsubara, Y. Koga, Y. Segawa, K. Murakami and K. Itami, *Nat. Catal.*, 2020, **3**, 710; (g) K. P. Kawahara, W. Matsuoka, H. Ito and K. Itami, *Angew. Chem., Int. Ed.*, 2020, **59**, 6383; (h) W. Matsuoka, H. Ito, D. Sarlah and K. Itami, *Nat. Commun.*, 2021, **12**, 3940; (i) W. Matsuoka, K. P. Kawahara, H. Ito, D. Sarlah and K. Itami, *J. Am. Chem. Soc.*, 2023, **145**, 658.
- 5 For selected reviews on on-surface synthesis, see: (a) S. Clair and D. G. De Oteyza, *Chem. Rev.*, 2019, **119**, 4717; (b) L. Grill and S. Hecht, *Nat. Chem.*, 2020, **12**, 115, For selected examples on on-surface synthesis, see: ; (c) J. Cai, P. Ruffieux, R. Jaafar, M. Bieri, T. Braun, S. Blankenburg, M. Muoth, A. P. Seitsonen, M. Saleh, X. Feng, K. Müllen and R. Fasel, *Nature*, 2010, **466**, 470; (d) H. Zhang, H. Lin, K. Sun, L. Chen, Y. Zagranyski, N. Aghdassi, S. Duhm, Q. Li, D. Zhong, Y. Li, K. Müllen, H. Fuchs and L. Chi, *J. Am. Chem. Soc.*, 2015, **137**, 4022; (e) S. Kawai, S. Saito, S. Osumi, S. Yamaguchi, A. S. Foster, P. Spijker and E. Meyer, *Nat. Commun.*, 2015, **6**, 8098; (f) P. Ruffieux, S. Wang, B. Yang, C. Sánchez-Sánchez, J. Liu, T. Dienel, L. Talirz, P. Shinde, C. A. Pignedoli, D. Passerone, T. Dumslaff, X. Feng, K. Müllen and R. Fasel, *Nature*, 2016, **531**, 489; (g) C. Moreno, M. Vilas-Varela, B. Kretz, A. Garcia-Lekue, M. V. Costache, M. Paradinas, M. Panighel, G. Ceballos, S. O. Valenzuela, D. Peña and A. Mugarza, *Science*, 2018, **360**, 199; (h) S. Mishra, T. G. Lohr, C. A. Pignedoli, J. Liu, R. Berger, J. I. Urgel, K. Müllen, X. Feng, P. Ruffieux and R. Fasel, *ACS Nano*, 2018, **12**, 11917; (i) J. Li, S. Sanz, N. Merino-Díez, M. Vilas-Varela, A. Garcia-Lekue, M. Corso, D. G. De Oteyza, T. Frederiksen, D. Peña and J. I. Pascual, *Nat. Commun.*, 2021, **12**, 5538.
- 6 (a) F. Würthner, C. R. Saha-Möller, B. Fimmel, S. Ogi, P. Leowanawat and D. Schmidt, *Chem. Rev.*, 2016, **116**, 962; (b) A. Borissov, Y. K. Maurya, L. Moshniaha, W.-S. Wong, M. Żyła-Karwowska and M. Stepień, *Chem. Rev.*, 2022, **122**, 565; (c) Q. Li, Y. Zhang, Z. Xie, Y. Zhen, W. Hu and H. Dong, *J. Mater. Chem. C*, 2022, **10**, 2411.
- 7 (a) J. P. Hill, W. Jin, A. Kosaka, T. Fukushima, H. Ichihara, T. Shimomura, K. Ito, T. Hashizume, N. Ishii and T. Aida, *Science*, 2004, **304**, 1481; (b) Y. Yamamoto, T. Fukushima, Y. Suna, N. Ishii, A. Saeki, S. Seki, S. Tagawa, M. Taniguchi, T. Kawai and T. Aida, *Science*, 2006, **314**, 1761; (c) W. Zhang, W. Jin, T. Fukushima, A. Saeki, S. Seki and T. Aida, *Science*, 2011, **334**, 340.
- 8 K. Takimiya, K. Bulgarevich, M. Abbas, S. Horiuchi, T. Ogaki, K. Kawabata and A. Ablat, *Adv. Mater.*, 2021, **33**, 2102914.
- 9 H.-A. Lin, Y. Sato, Y. Segawa, T. Nishihara, N. Sugimoto, L. T. Scott, T. Higashiyama and K. Itami, *Angew. Chem., Int. Ed.*, 2018, **57**, 2874.
- 10 S. Zhang, W. Li, J. Luan, A. Srivastava, V. Carnevale, M. L. Klein, J. Sun, D. Wang, S. P. Teora, S. J. Rijpkema, J. D. Meeldijk and D. A. Wilson, *Nat. Chem.*, 2023, **15**, 240.
- 11 (a) Y.-Z. Tan, B. Yang, K. Parvez, A. Narita, S. Osella, D. Beljonne, X. Feng and K. Müllen, *Nat. Commun.*, 2013, **4**, 2646; (b) Y.-M. Liu, H. Hou, Y.-Z. Zhou, X.-J. Zhao, C. Tang, Y.-Z. Tan and K. Müllen, *Nat. Commun.*, 2018, **9**, 1901.
- 12 (a) M. N. Eliseeva and L. T. Scott, *J. Am. Chem. Soc.*, 2012, **134**, 15169; (b) R. Yamaguchi, S. Hiroto and H. Shinokubo, *Org. Lett.*, 2012, **14**, 2472; (c) K. Kawasumi, Q. Zhang, Y. Segawa, L. T. Scott and K. Itami, *Nat. Chem.*, 2013, **5**, 739; (d) Y. Segawa, T. Maekawa and K. Itami, *Angew. Chem., Int. Ed.*, 2015, **54**, 66; (e) K. Kato, H.-A. Lin, M. Kuwayama, M. Nagase, Y. Segawa, L. T. Scott and K. Itami, *Chem. Sci.*, 2019, **10**, 9038; (f) I. A. Stepek and K. Itami, *ACS Mater. Lett.*, 2020, **2**, 951.
- 13 R. C. Larock, M. J. Doty, Q. Tian and J. M. Zenner, *J. Org. Chem.*, 1997, **62**, 7536.
- 14 For selected reviews on biaryl synthesis by C-H arylation, see: (a) D. Alberico, M. E. Scott and M. Lautens, *Chem. Rev.*, 2007, **107**, 174; (b) L.-C. Campeau, D. R. Stuart and K. Fagnou, *Aldrichimica Acta*, 2007, **40**, 35; (c) X. Chen, K. M. Engle, D. Wang and J.-Q. Yu, *Angew. Chem., Int. Ed.*, 2009, **48**, 5094; (d) L. Ackermann, R. Vicente and A. R. Kapdi, *Angew. Chem., Int. Ed.*, 2009, **48**, 9792; (e) J. Yamaguchi, A. D. Yamaguchi and K. Itami, *Angew. Chem., Int. Ed.*, 2012, **51**, 8960; (f) M. Simonetti, D. M. Cannas and I. Larrosa, *Adv. Organomet. Chem.*, 2017, **67**, 299; (g) W. Hagui, H. Doucet and J.-F. Soulé, *Chem*, 2019, **5**, 2006; (h) J. Grover, G. Prakash, N. Goswami and D. Maiti, *Nat. Commun.*, 2022, **13**, 1085.
- 15 (a) L.-C. Campeau, M. Parisien, M. Leblanc and K. Fagnou, *J. Am. Chem. Soc.*, 2004, **126**, 9186; (b) M. Parisien, D. Valette and K. Fagnou, *J. Org. Chem.*, 2005, **70**, 7578; (c) L.-C. Campeau, P. Thansandote and K. Fagnou, *Org. Lett.*, 2005, **7**, 1857; (d) L.-C. Campeau, M. Parisien, A. Jean and K. Fagnou, *J. Am. Chem. Soc.*, 2006, **128**, 581; (e) M. Lafrance, D. Lapointe and K. Fagnou, *Tetrahedron*, 2008, **64**, 6015; (f) D. Lapointe and K. Fagnou, *Chem. Lett.*, 2010, **39**, 1118.
- 16 C. Pinilla, V. Salamanca, A. Lledós and A. C. Albéniz, *ACS Catal.*, 2022, **12**, 14527.



- 17 Y. Morinaka, H. Ito, K. J. Fujimoto, T. Yanai, Y. Ono, T. Tanaka and K. Itami, *Angew. Chem., Int. Ed.*, 2024, **63**, e202409619.
- 18 S. Hashimoto, T. Ikuta, K. Shiren, S. Nakatsuka, J. Ni, M. Nakamura and T. Hatakeyama, *Chem. Mater.*, 2014, **26**, 6265.
- 19 V. Diemer, H. Chaumeil, A. Defoin, P. Jacques and C. Carré, *Tetrahedron Lett.*, 2005, **46**, 4737.
- 20 (a) H. Yamagishi, S. Nakajima, J. Yoo, M. Okazaki, Y. Takeda, S. Minakata, K. Albrecht and K. Yamamoto, *Commun. Chem.*, 2020, **3**, 118; (b) T. Ono and Y. Hisaeda, *Symmetry*, 2020, **12**, 1903.

